Hepatology Research 2007; 37: 1068–1079 doi: 10.1111/j.1872-034X.2007.00162.x

Original Article

Hepatic differentiation of human bone marrow-derived UE7T-13 cells: Effects of cytokines and CCN family gene expression

Takashi Shimomura,[1] Yoko Yoshida,[1] Tomohiko Sakabe,[1] Kyoko Ishii,[1] Kazue Gonda,[1] Rie Murai,[1] Kazuko Takubo,[2] Hiroyuki Tsuchiya,[1] Yoshiko Hoshikawa,[1] Akihiro Kurimasa,[1] Ichiro Hisatome,[3] Taro Uyama,[4] Akihiro Umezawa[4] and Goshi Shiota[1]

[1]*Division of Molecular and Genetic Medicine, Department of Genetic Medicine and Regenerative Therapeutics, Graduate School of Medicine, Tottori University,* [2]*Division of Oral and Maxillofacial Biopathological Surgery, Department of Medicine of Sensory and Motor Organs, Faculty of Medicine, Tottori University,* [3]*Division of Regenerative Therapeutics, Graduate School of Medicine, Tottori University, Tottori, and* [4]*Department of Reproductive Biology and Pathology, National Research Institute for Child Health and Development, Tokyo, Japan*

Aim: Bone marrow-derived mesenchymal stem cells (MSC) are expected to be an excellent source of cells for transplantation. We aimed to study the culture conditions and involved genes to differentiate MSC into hepatocytes.

Methods: The culture conditions to induce the efficient differentiation of human bone marrow-derived UE7T-13 cells were examined using cytokines, hormones, 5-azacytidine and type IV collagen.

Results: We found that combination of acidic fibroblast growth factor (aFGF), basic fibroblast growth factor (bFGF) and hepatocyte growth factor (HGF) with type IV collagen coating induced hepatic differentiation of UE7T-13 cells at over 30% frequency, where expression of albumin mRNA was increased over 20-fold. The differentiated cells had functions of albumin production, glycogen synthesis and urea secretion as well as expressing hepatocyte-specific genes. In addition, these cells have binuclear and cuboidal morphology, which is a characteristic feature of hepatocytes. During hepatic differentiation, UE7T-13 cells showed depressed expression of *WISP1* and *WISP2* genes, members of the CCN family. Conversely, knockdown of *WISP1* or *WISP2* gene by siRNA stimulated hepatic differentiation. The effect of aFGF/bFGF/HGF/type IV collagen coating and WISP1-siRNA on hepatic differentiation was additive.

Conclusion: The present study suggests that aFGF/bFGF/HGF/type IV collagen coating is the efficient condition for hepatic differentiation of UE7T-13 cells, and that WISP1 and WISP2 play an important role in hepatic transdifferentiation of these cells.

Key words: bone marrow, CCN family, hepatocytes, mesenchymal stem cells, transdifferentiation

INTRODUCTION

BONE MARROW IS a reservoir of various stem cells, including hematopoietic stem cells (HSC) and mesenchymal stem cells (MSC). Bone marrow cells have great potential as therapeutic agents, as they are easy to isolate and can be expanded from patients without serious ethical and technical problems. In addition, the use of autologous transplantation of bone marrow-derived cells can prevent immune rejection. Thus, bone marrow-derived cells have several advantages for the development of regenerative medicine.

It has long been thought that the differentiation potential of adult stem cells is limited to their germ layer of origin, but recent studies have demonstrated that adult stem cells are more plastic than once believed.[1–3] Bone marrow cells have been reported to differentiate into hepatocytes.[2,3] The frequency of hepatocytes that were considered to be bone marrow derived varied from 0.5% to 8% in transplanted patients.[1,4,5] *In vivo*

Correspondence: Professor Goshi Shiota, Division of Molecular and Genetic Medicine, Department of Genetic Medicine and Regenerative Therapeutics, Graduate School of Medicine, Tottori University, Tottori, Japan. Email: gshiota@grape.med.tottori-u.ac.jp
Received 15 April 2007; revision 2 May 2007; accepted 3 May 2007.

transplantation studies showed that MSC can differentiate into endodermal cell types as well as having many mesodermal and neuroectodermal characteristics.[6] Bone marrow-derived MSC can differentiate into hepatocytes.[7,8] Hence, human MSC may serve as a source of cell therapy for liver diseases.

An alternative mechanism for plasticity could be the fusion of a bone marrow-derived cell with a non-hematopoietic cell to form a heterokaryon, thereby converting the gene expression pattern of the original bone marrow cell type to that of the fusion partner.[9] However, it remains to be clarified whether cell fusion may generate functionally intact hepatocytes that may not carry a high risk for transformation. In this context, the differentiated hepatocytes from bone marrow cells *in vitro*, which do not mediate cell fusion, are a reliable cell source for regenerative medicine. We therefore attempted to identify the efficient culture conditions and associated genes which regulate hepatic differentiation of human bone marrow-derived cells.

METHODS

Materials

ACIDIC AND BASIC fibroblast growth factor (aFGF, bFGF, respectively) and hepatocyte growth factor (HGF) were obtained from PeproTech EC (London, UK). Oncostatin M (OSM) and leukemia inhibitory factor (LIF) were purchased from DIACLONE Research (Cedex, France) and Alomone Labs (Jerusalem, Israel), respectively. Dexamethasone (Dex) and 5-azacytidine (5-aza) were obtained from Nacalai Tesque (Kyoto, Japan). ITS$^+$ premix (6.25 μg/mL insulin, 6.25 μg/mL transferrin, 6.25 ng/mL selenious acid, 1.25 mg/mL bovine serum albumin, 5.35 mg/mL linoleic acid) and type IV collagen were obtained from Becton Dickinson (Franklin Lakes, NJ, USA).

In vitro hepatic differentiation

Human bone marrow-derived mesenchymal stem cells (hMSC), the life span of which was prolonged by infecting retrovirus encoding human papillomavirus E7 and human telomerase reverse transcriptase (hTERT), designated UE7T-13 cells,[10,11] were used in the present study. To induce hepatic differentiation of UE7T-13 cells, the combined effects of cytokines, 5-aza and type IV collagen coating were examined. First, the effects of cytokines (20 ng/mL aFGF, 10 ng/mL bFGF, 20 ng/mL HGF, 20 ng/mL OSM, 10 ng/mL LIF, 0.5 μM Dex, 50 mg/mL ITS) with or without 10 μM 5-aza treatment were examined.[12–14] UE7T-13 cells were plated on 6-well plates (BD Falcon, Tokyo, Japan) at 9.0×10^3 cells/cm^2 (Fig. 1a). At 6 days, the cells were exposed to 10 μM 5-aza for 24 h. At 7 days, UE7T-13 cells were cultured for 3 weeks in Dulbecco's modified Eagle's medium (DMEM; IWAKI, Tokyo, Japan) containing 10% fetal bovine serum (FBS) and cytokines. Medium changes were performed twice a week, and the cells were replated at 9.0×10^3 cells/cm^2 every week. Second, the combined effects of cytokines, 5-aza and type IV collagen coating on hepatic differentiation were examined with the same schedule (Fig. 1a). Hepatogenesis was assessed by reverse transcription-polymerase chain reaction (RT-PCR) for hepatocyte-specific genes, periodic acid–Schiff staining, albumin staining and urea assay.

Total RNA isolation and real-time RT-PCR

Total RNA was extracted from UE7T-13 cells at 0, 1, 2, 3 and 4 weeks after starting culture using RNAgents Total RNA Isolation System (Promega, Madison, WI, USA). After treatment with DNase (Nippongene, Toyama, Japan), the mRNA was reverse transcribed to cDNA using SuperScript First-Strand Synthesis System for RT-PCR (Invitrogen, Carlsbad, CA, USA).

For RT-PCR, cDNA was amplified using a PCR Thermal Cycler Dice (TaKaRa Bio, Kyoto, Japan) at 94°C for 30 s, the indicated annealing temperature for 30 s, and 72°C for 30 s for 35 cycles. After initial denaturation at 94°C for 5 min, cDNAs of albumin, glutamine synthetase (GS), cytokeratin 18 (CK18), α-fetoprotein (AFP), tyrosine-aminotransferase (TAT), tryptophan 2,3-dioxygenase (TO), glucose-6-phosphatase (G6P), cytochrome p4502B6 (CYP2B6), hepatic nuclear factor 4 (HNF4), c-mpl, c-met, c-kit, LIF receptor, FGF receptor 1, OSM receptor β and glyceraldehyde-3-phosphate dehydrogenase (GAPDH) were amplified using the primers (Table 1). The intensity of the bands was measured by ImageJ (http://rsb.info.nih.gov/ij/). After being normalized by GAPDH, the intensity was expressed as a ratio of expression level at 0 day.

Real-time RT-PCR was done using cDNA and SYBR Green I (Roche, Basel, Switzerland) in a LightCycler 1.5 (Roche Diagnostics, Osaka, Japan). The condition of quantitative RT-PCR was an initial incubation at 95°C for 10 min, followed by 45 cycles at 95°C for 0 s, the indicated annealing temperature for 5 s, and 72°C for product size/25 s. The primers are listed in Table 2. The authenticity and size of the PCR products were confirmed by using a melting curve analysis by LightCycler Software Version 3.5 (Roche Diagnostics) and a gel

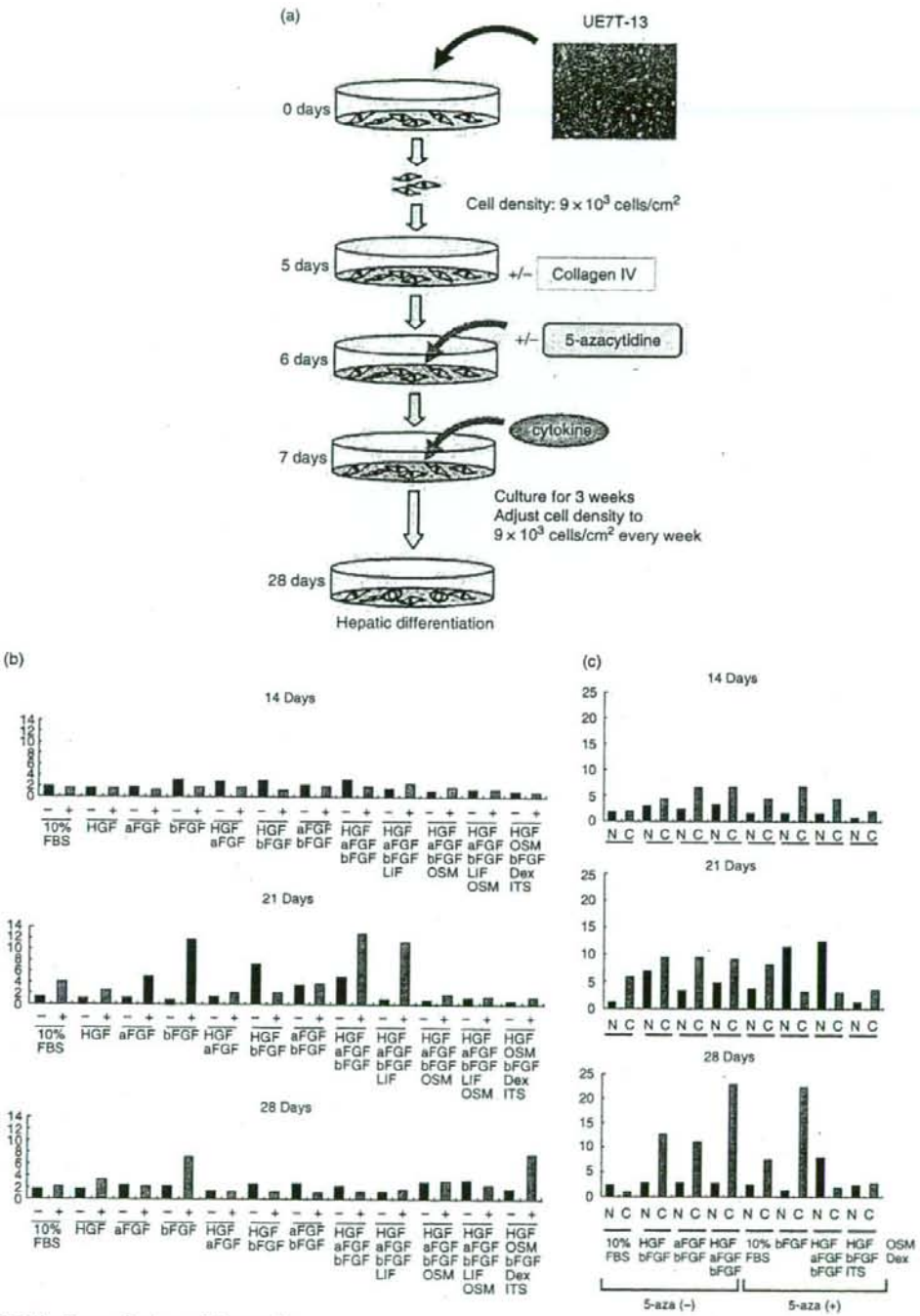

Table 1 Primers for reverse transcription–polymerase chain reaction

		Size (bp)	Temp. (°C)
Albumin	Forward TTGGAAAAATCCCACTGCAT Reverse CTCCAAGCTGCTCAAAAAGC	350	58
GS	Forward GTCAAGATTGCGGGGACTAA Reverse TACGATTGGCTACACCACCA	397	58
CK 18	Forward GAGATCGAGGCTCTCAAGGA Reverse CAAGCTGGCCTTCAGATTTC	357	58
AFP	Forward TGCCAACTCAGTGAGGACAA Reverse TCCAACAGGCCTGAGAAATC	356	58
TAT	Forward TGAGCAGTCTGTCCACTGCCT Reverse ATGTGAATGAGGAGGATCTGAG	358	56
TO	Forward ATACAGAGACTTCAGGGAGC Reverse TGGTTGGGTTCATCTTCGGTATC	299	54
G6P	Forward GCTGGAGTCCTGTCAGGCATTGC Reverse TAGAGCTGAGGCGGAATGGGAG	350	56
CYP2B6	Forward GACGCTACGTTTCAGTCTTTC Reverse GCTGAATACCACGCCATAG	204	54
HNF4	Forward CCAAGTACATCCCAGCTTTC Reverse TTGGCATCTGGGTCAAAG	295	56
c-mpl	Forward TGGAGATGCAGTGGCACTTG Reverse GAGAACTGTGGGGTCTGTAGT	204	57
c-met	Forward ACTCCCCCTGAAAACCAAAGCC Reverse GGCTTACACTTCGGGGCACTTAC	536	60
c-kit	Forward TGTGATGATTCTGACCTACA Reverse GAATCACGTTTTCTTCTCAA	447	48
LIFR	Forward GAAAACTGTAAAGCATTACA Reverse AGAGTCTGGAGACACTAA	504	46
FGFR1	Forward CGCTCTAGAGCAGAACTGGGATGTGGGGCTG Reverse CTCGGATCCAGGGCTTCCAGAACGGTC	832	60
OSMRβ	Forward GTGTGGGTGCTTCTCCTGCTTCTGTA Reverse TCTGTGCTAATGACTGTGCTTGTGGT	235	56
GAPDH	Forward GTCTTCTCCACCATGGAGAAGGCT Reverse CATGCCAGTGAGCTTCCCGTTCA	395	60

analysis. mRNA level was normalized using β-actin as an internal control.

DNA microarrays and transfection of siRNA

RNA was extracted from the UE7T-13 cells that were cultured in DMEM containing 10% FBS, 20 ng/mL HGF, 20 ng/mL aFGF and 10 ng/mL bFGF on a type IV collagen dish for 7 days and those that were cultured in 10% FBS on a non-coated dish for 7 days. DNA microarray was performed by using the pathway-specific microarray using Oligo GEArray Human Signal Transduction PathwayFinder™ M (SuperArray Bioscience,

Figure 1 Culture schedule and albumin mRNA expression levels. (a) Induction schedule for hepatic differentiation. UE7T-13 cells were plated at 9×10^3 cells/cm^2 for 5 days. After treatment with or without 5-aza for 24 h, the cells were cultured in the medium containing several kinds of cytokines for 3 weeks. The cells were replated at 9×10^3/cm^2 every week. (b) Expression levels of albumin mRNA at 14, 21 and 28 days in 24 different conditions. Levels of albumin mRNA were expressed as the ratio to GAPDH mRNA. (c) Expression levels of albumin mRNA at 14, 21 and 28 days in 16 different conditions. Levels of albumin mRNA were expressed as the ratio to GAPDH mRNA. aFGF, acidic fibroblast growth factor; bFGF, basic fibroblast growth factor; C, type IV collagen coating; d, days; Dex, dexamethasone; HGF, hepatocyte growth factor; LIF, leukemia inhibitory factor; N, non-coating; OSM, oncostatin M.

Table 2 Primers of real-time reverse transcription–polymerase chain reaction for *CCN* family genes

Gene	Sequences	Size (bp)	Temp.† (°C)
CCN1	Forward CCGAGGTGGAGTTGACGAGAAA Reverse TCTTTCACAAGGCGGCACTCAG	226	65
CCN2	Forward CACCAGCATGAAGACATACCG Reverse CGTCAGGGCACTTGAACTCCA	110	62
CCN3	Forward GGTGCCTGGAGAGTGCTGTG Reverse GGCCTGTAAGCTGCAAGGGTAA	87	64
CCN4	Forward GGAGGCTGCCATCTGTGACC Reverse CACACACTCCTATTGCGTACCTCG	83	60
CCN5	Forward AGTTTTCTGGCCTTGTCTCT Reverse AGAAGCGGTTCTGGTTGGAC	129	62
CCN6	Forward AGTGTGTGCATACCTTGTAGCTG Reverse GGGTTGGGCTGAAACACTTGG	81	65
β-Actin	Forward CGTACAGGTCTTTGCGGATGTC Reverse CACTCTTCCAGCCTTCCTTCC	103	56

†Annealing temperature.

Frederick, MD, USA), which profiles 113 genes representative of 18 signal transduction pathways, according to the manufacturer's instruction. Briefly, cRNA was prepared from cDNA which was reverse transcribed from RNA by a TrueLabeling-AMP Linear RNA Amplification Kit and purified. Hybridization was done overnight using a membrane (Signal Transduction PathwayFinder Oligo GEArray in HybTube Format; Cosmo Bio, Tokyo, Japan). Chemifluorescence was detected by Luminescent Image Analyzer LAS-1000plus (Fujifilm, Tokyo, Japan) and GEArray Expression Analysis Suite (SuperArray Bioscience).

siRNA transfection experiments were performed with double stranded RNAs which were purchased from Hokkaido System Science (Sapporo, Japan). WISP1-specific siRNA-1 and -2 sense-orientation strands with the following sequences (5′-GCCAGGUCCUAUGGA UUAAdTdT-3′) and 5′-CUCGGAUCUCCAAUGUUAAd TdT-3′) were selected. WISP2-specific siRNA-1 and -2 sense-orientation strands with the following sequences (5′-GGUGCGUACCCAGCUGUGCCCGACAdAdG-3′) and (5′-GACCCACCUCCUGGCCUUCUCCCUCdAdG-3′) were also selected. A non-silencing control siRNA (control siRNA Alexa Fluor 488; Invitrogen KK Japan, Tokyo, Japan) sense-orientation strand with the following sequence (5′- UUCUCCGAACGUGUCACGUdTdT-3′) was used. Then, 9×10^3 cells/cm^2 in 24-well plates (BD Falcon) were transfected with RNAiFect Tranfection Reagent (Qiagen) using 1 μg siRNA according to the manufacturer's instruction. Transfection efficiency in cells was determined with fluorescein isothiocyanate (FITC)-labeled siRNA (control siRNA Alexa Fluor 488) and evaluated by cell counting using a fluorescent microscope (Olympus IX71; Olympus, Tokyo, Japan) to be 90–95% after 24 and 48 h. To examine the effect of siRNA on cell differentiation, WISP1-specific siRNA2 and WISP2-specific siRNA2 were transfected with UE7T-13 cells weekly up to 4 weeks after starting cell culture.

Immunocytochemistry, periodic acid–Schiff stain for glycogen

Cells were fixed overnight with 4% formaldehyde at 4°C, and permeabilized with 0.1% Triton X-100 (Wako Pure Chemical Industries, Osaka, Japan) for 10 min. Slides were incubated with mouse primary antibody against human albumin (1:1000) (Sigma-Aldrich, St Louis, MO, USA) at 37°C for 1 h, and then stained with the avidin–biotin–peroxidase complex (Vector Laboratories, Burlingame, CA, USA).

Culture dishes were fixed in 4% formaldehyde, permeabilized with 0.1% Triton X-100 for 10 min and either were not incubated or were incubated with α-amylase (Nacalai Tesque) for 3 h at 37°C. Samples were then oxidized in 1% periodic acid for 5 min, rinsed three times in deionized (d) H_2O treated with Schiff's reagent (Nacalai Tesque) for 15 min, and rinsed in dH_2O three times. Samples were counterstained with Mayer's hematoxylin for 1 min and assessed under a light microscope (Olympus BX41; Olympus). The percentages of albumin-positive or periodic acid–Schiff (PAS)-positive cells were expressed as the number of positive cells divided by the total cell number of eight randomly selected fields.

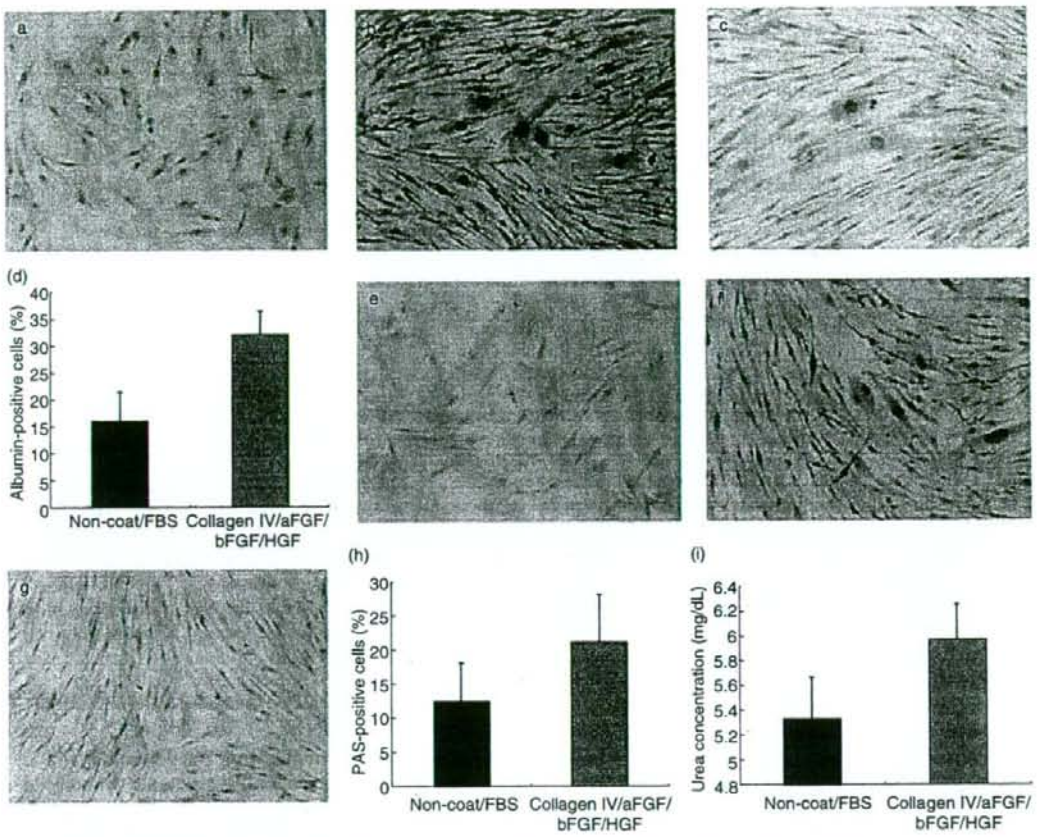

Figure 2 Functional assays of hepatocyte-like cells. (a) UE7T-13 cells (albumin staining, original magnification ×200). (b) UE7T-13 cells cultured in HGF/aFGF/bFGF on type IV collagen-coated dish for 21 days (albumin staining, original magnification ×200). Hepatocyte-like cells which express much albumin appear. (c) UE7T-13 cells cultured in 10% fetal bovine serum (FBS) on non-coated dish for 21 days (albumin staining, original magnification ×200). (d) Percentages of albumin-positive cells cultured in HGF/aFGF/bFGF on type IV collagen-coated dish and 10% FBS on non-coated dish. Data are expressed as mean ± SD of five experiments. (e) UE7T-13 cells (periodic acid–Schiff [PAS] staining, original magnification ×200). (f) UE7T-13 cells cultured in HGF/aFGF/bFGF on type IV collagen-coated dish for 21 days (PAS staining, original magnification ×200). Hepatocyte-like cells which store glycogen appear. (g) UE7T-13 cells cultured in 10% FBS on non-coated dish for 21 days (PAS staining, original magnification ×200). (h) Percentages of PAS staining-positive cells cultured in HGF/aFGF/bFGF on type IV collagen-coated dish and 10% FBS on non-coated dish. Data are expressed as mean ± SD of five experiments. (i) Urea production in the media of the cells cultured in HGF/aFGF/bFGF on type IV collagen-coated dish and 10% FBS on non-coated dish. Data are expressed as mean ± SD of five experiments. aFGF, acidic fibroblast growth factor; bFGF, basic fibroblast growth factor; HGF, hepatocyte growth factor.

Urea assay

UE7T-13 cells in 24-well plates (BD Falcon) were cultured in 5 mM ammonium chloride (Nacalai Tesque) for 48 h, and then urea concentrations were determined by QuantiChrom Urea Assay Kit (BioAssay Systems, Hayward, CA, USA) according to the manufacturer's instruction, and were analyzed with HITACHI U-1500 (Hitachi, Tokyo, Japan). The data were expressed as mean ± SD of five experiments.

RESULTS

Optimal conditions for hepatic differentiation

UE7T-13 CELLS, which originally have the ability of osteogenic, chondrogenic, and adiopogenic differentiation, can be differentiated into cardiomyocytes and neurons;[12,15] however, hepatic differentiation ability has been unknown. UE7T-13 cells strongly express c-kit, c-met, FGF receptor 1, and OSM receptor, but weakly express LIF receptor β (data not shown). To determine the optimal method of hepatic differentiation, the first experiments were done in 24 culture conditions using HGF, aFGF, bFGF, LIF, OSM, Dex, ITS and 5-aza (Fig. 1b). UE7T-13 cells scarcely express albumin mRNA at 0 day. In the absence of 5-aza, higher expression of albumin mRNA was observed in the conditions of HGF/bFGF, aFGF/bFGF and HGF/aFGF/bFGF at 21 days; however, expression level decreased at 28 days. In the presence of 5-aza, albumin mRNA was strongly expressed in culture conditions of aFGF, bFGF, HGF/aFGF/bFGF and HGF/aFGF/bFGF/LIF at 21 days, and was still higher in bFGF and HGF/OSM/bFGF/Dex/ITS at 28 days. Overall expression of albumin mRNA was decreased at 28 days (Fig. 1b). Then, the cells were examined for hepatogenesis on type IV collagen as scaffold protein, because a type IV collagen coating stimulated colony formation of mouse hepatic progenitor cells.[16] The combined effects of cytokines, 5-aza and type IV collagen were examined in 16 types of culture conditions (Fig. 1c). In the presence of type IV collagen, the cells expressed a higher level of albumin mRNA; however, in the absence of type IV collagen they did not. At 28 days, the highest expression of albumin mRNA was obtained in the cells cultured in the condition of HGF/aFGF/bFGF/collagen coating, and higher expression was observed in the condition of bFGF/5-aza/collagen coating.

By RT-PCR analysis, expression of other hepatocyte-specific genes such as *AFP*, *K-18*, *G6P*, *TAT*, GS and *TO* was examined at 28 days. Expression of these genes tended to be higher in 5-aza-treated cells, especially in the cells treated with bFGF/5-aza/collagen coating, and was also higher in the condition of HGF/aFGF/bFGF/collagen coating. Expression of CYP2B6 and HNF4 was not observed until 4 weeks after induction (data not shown).

Table 3 DNA microarray analysis

Symbol	Pathway	Group 1/Group 2
Upregulated genes		
BCL2A1	Survival (NF-κB)	2.970779996
CCL20	NF-κB	1.978631867
FOXA2	Hedgehog	1.504629504
GREB1	Estrogen	1.505453786
IL1A	NF-κB	1.827547367
IL4	Jak-Stat	1.752106063
NOS2A	Jak-Stat	1.536994317
LEP	Insulin	1.944428028
PECAM1	NF-κB	1.576490344
PGR	Estrogen	1.581404729
PTGS2	Phospholipase C	5.000349291
RBP1	Retinoic acid	1.646096039
SELE	LDL	2.16645166
TMEPAI	Androgen	1.953435518
TRIM25	Estrogen	4.422090754
VEGF	Wnt	2.308966453
WSB1	Hedgehog	1.695788997
Downregulated genes		
ATF2	Stress	0.535377059
BAX	p53	0.516648555
BCL2	Estrogen	0.579983284
BIRC1	Survival (NF-κB)	0.553646131
BIRC2	Survival (NF-κB)	0.645158295
BIRC5	Wnt	0.505786989
BMP4	Hedgehog	0.585645362
BRCA1	Estrogen	0.585153761
CD5	NFAT	0.621715546
CDK2	Androgen	0.565415139
CDKN1C	TGF-beta	0.557206377
CDKN2A	TGF-beta	0.50807409
CDKN2B	TGF-beta	0.480227082
CDX1	Retinoic acid	0.547114338
C/EBPβ	Insulin	0.600885902
CSN2	Jak-Stat	0.562621027
CTSD	Estrogen	0.491377292
CXCL12	Estrogen	0.215851667
EN1	Hedgehog	0.499769336
HK2	Insulin	0.62796643
HSPCA	Stress	0.572358328
IGFBP3	p53	0.501512431
IKBKB	NF-κB	0.419132357
TANK	NF-κB	0.631916221
FAS	p53	0.593650284
FASLG	NFAT	0.262290028
TP53	p53	0.128023898
WISP1	Wnt	0.212766767
WISP2	Wnt	0.102305807

LDL, low-density lipoprotein; NF-κB, nuclear factor kappa B; TGF, tumor growth factor.

Immunocytochemistry of the differentiated cells

While undifferentiated UE7T-13 cells did not express albumin (Fig. 2a), Four-week-culture condition of HGF/aFGF/bFGF/collagen coating induced many albumin-positive cells (Fig. 2b). Some round or oval-shaped cells appeared in fibroblastic bipolar MSC, and these cells began to lose their edges and progressed toward the polygonal morphology of hepatocytes in a time-dependent manner. The culture condition of 10% FBS/non-coating induced far fewer hepatocyte-like cells (Fig. 2c). The rate of albumin positivity was 32% by HGF/aFGF/bFGF/collagen coating, whereas only 15% of cells were positive for albumin in 10% FBS/non-coated culture (Fig. 2d). The presence of glycogen in many cells, which were examined by PAS staining, was accelerated by HGF/aFGF/bFGF/collagen coating, while not as many cells were stained by 10% FBS/non-coating (Fig. 2e–h). When pretreated with α-amylase to digest glycogen, the cells were negative for glycogen (data not shown). Interestingly, binuclear cells, which are a typical feature of hepatocytes, appeared (Fig. 2f). In addition, HGF/aFGF/bFGF/collagen-coated cells synthesize significantly higher amounts of urea than 10% FBS/non-coated cells (Fig. 2i).

Genes which are associated with hepatic differentiation

To identify the genes which are induced by optimal condition, a pathway-specific microarray was performed. Of 113 genes, 17 genes were upregulated and 30 genes were downregulated (Table 3). Of these genes, expression of *WISP1* (Wnt-1 induced secreted protein 1, CCN4) and *WISP2* (Wnt-1 induced secreted protein 2, CCN5) genes was reduced to 21% and 10% of the control condition, respectively. Wnt signal regulates self-renewability of hematopoietic stem cells[11] and CCN family proteins are associated with cell growth and differentiation.[17] Indeed, it has been reported that *WISP1* is an osteoblastic regulator during skeletal development[18] and CCN1 plays an important role in osteoblast differentiation.[16] Expression of *WISP1* was greatly reduced in HGF/aFGF/bFGF/

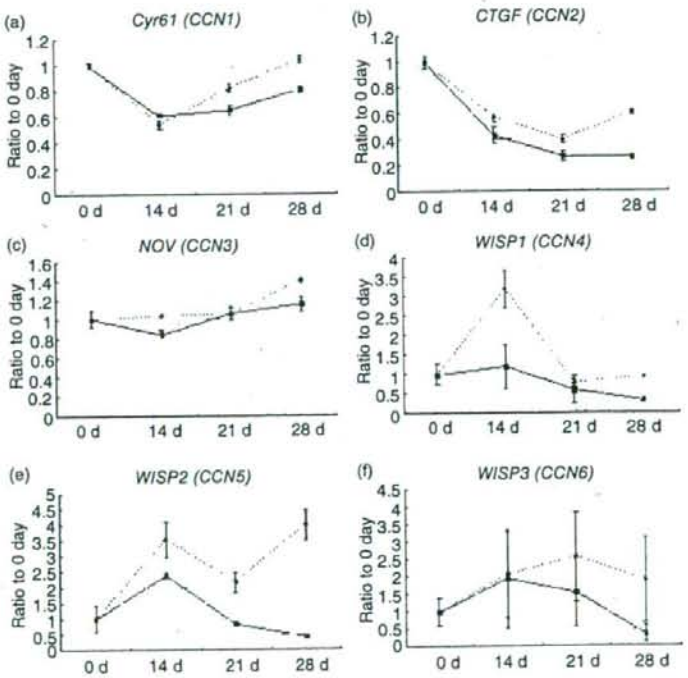

Figure 3 Serial analysis of CCN family mRNA expression. (a) *Cyr61* (*CCN1*). Data are expressed as mean ± SD of five experiments. (b) *CTGF* (*CCN2*). (c) *NOV* (*CCN3*). (d) *WISP1* (*CCN4*). (e) *WISP2* (*CCN5*). (f) *WISP3* (*CCN6*). (·····), Control; (——), HGF/aFGF/bFGF/collagen coating.

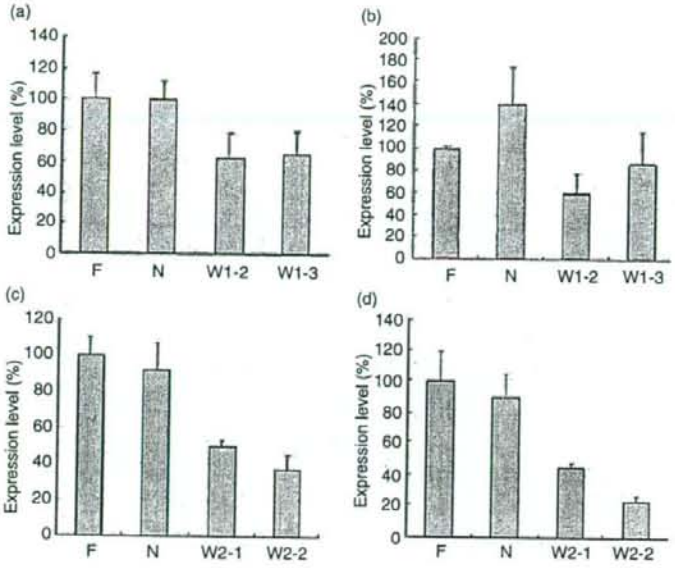

Figure 4 Expression level of WISP1 and WISP2 mRNA at 24 and 48 h after siRNA transfection. (a) Expression of WISP1 mRNA at 24 h after transfection. siRNAs include three types of WISP1-siRNA and two types of WISP2-siRNA. F, 10% fetal bovine serum (FBS) only; N, non-silencing control siRNA; W1-2, WISP1-siRNA no. 2; W1-3, WISP1-siRNA no. 3. Data are expressed as mean ± SD of five experiments. (b) Expression of WISP1 mRNA at 48 h after transfection. (c) Expression of WISP2 mRNA at 24 h after transfection. F, 10% FBS only; N, non-silencing control siRNA; W2-1, WISP2-siRNA no. 1; W2-2, WISP1-siRNA no. 2. (d) Expression of WISP2 mRNA at 48 h after transfection.

collagen-coated cells at 14 days, and was still lower at 28 days although the difference was small (Fig. 3d). Reduced expression of *WISP2* was observed at 14, 21 and 28 days (Fig. 3e). Expression of CCN1, 2, 3 and 6 was not changed by the condition of HGF/aFGF/bFGF/collagen coating (Fig. 3a–c,f).

Knockdown of *WISP1* and *WISP2*

By siRNA transfection of W1-2, expression of *WISP1* was reduced to about 60% and after 24 and 48 h (Fig. 4a,b), respectively. W1-3 transfection caused reduction of *WISP2* mRNA to 63% after 24 h and 88% after 48 h (Fig. 4a,b). Expression of *WISP2* by W2-1 was decreased to 50% and 45% after 24 and 48 h, respectively (Fig. 4c,d). W2-2 reduced *WISP2* mRNA to 38% at 24 h and to 22% at 48 h (Fig. 4c,d). The culture condition of HGF/aFGF/bFGF/collagen coating reduced *WISP1* mRNA and *WISP2* mRNA (Fig. 5a,b). siRNA specific for *WISP1* decreased expression of WISP1 mRNA in the cells of both 10% FBS/non-coat and HGF/aFGF/bFGF/collagen coating (Fig. 5a). siRNA specific for WISP2 also inhibited expression of WISP2 mRNA in both 10% FBS/non-coating and HGF/aFGF/bFGF/collagen coating (Fig. 5b). In 10% FBS/non-coated cells, WISP1-siRNA and WISP2-siRNA increased albumin-positive cells ($P < 0.01$ and $P < 0.05$, respectively, Fig. 6c). The effect of WISP2-siRNA and HGF/aFGF/bFGF/collagen-coating condition was additive in increasing albumin-positive cells ($P < 0.01$, Fig. 5c). However, the effect of WISP1-siRNA with HGF/aFGF/bFGF/collagen coating was not different from that with HGF/aFGF/bFGF/collagen coating. The PAS-positive cells were increased by WISP1-siRNA and WISP2-siRNA, compared with control siRNA ($P < 0.01$, each, Fig. 5d). Transfection with WISP2-siRNA in combination with HGF/aFGF/bFGF/collagen-coated condition increased the PAS-positive cells, compared with HGF/aFGF/bFGF/collagen-coated condition ($P < 0.01$); however, WISP1-siRNA did not. Transfection with WISP1-siRNA or WISP2-siRNA induced greater urea production ($P < 0.01$, each, Fig. 5e), and the bigger effect was observed in combination of HGF/aFGF/bFGF/collagen coating with WISP1-siRNA or WISP2-siRNA ($P < 0.01$, each).

The effects of WISP1-siRNA and WISP2-siRNA on changes of morphology were evident; the cells became extended, round and oval-shaped cells by WISP1-siRNA/non-coat (Fig. 6a), and the cell shape became more extended by WISP2-siRNA (Fig. 6b), while many cells remained fibroblastic shaped in 10% FBS/non-coated condition (Fig. 6c). Combination of WISP1-siRNA with HGF/aFGF/bFGF/collagen-coated condition promoted hepatic morphogenesis (Fig. 6d). Albumin

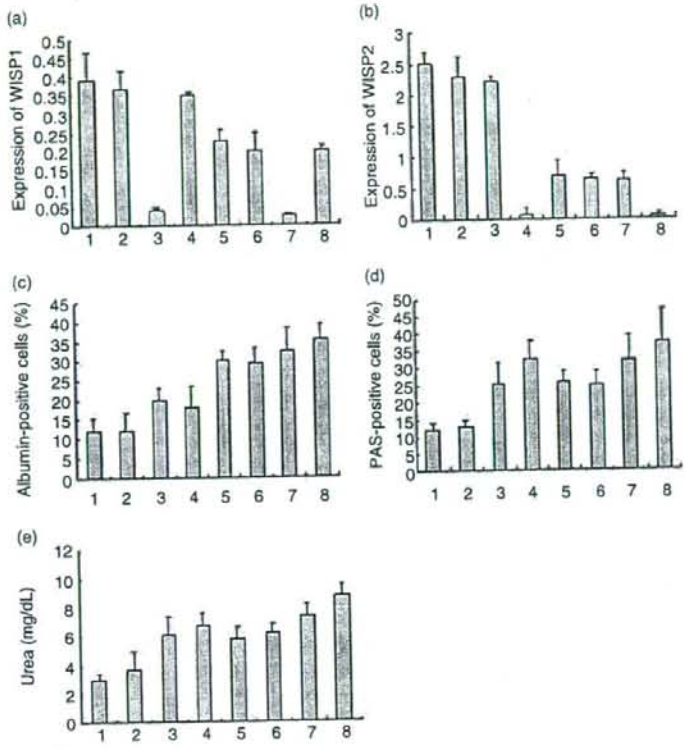

Figure 5 Effects of knockdown of WISP1 and WISP2 on hepatic differentiation. (a) Expression level of WISP1 mRNA at 28 days after weekly transfection of WISP1-siRNA.1, 2, 3 and 4 represent the condition of 10% fetal bovine serum (FBS)/non-coat, and 5, 6, 7 and 8 represent the condition of HGF/aFGF/bFGF/collagen coating. 1 and 5, no transfection; 2 and 6, transfection with non-silencing control siRNA; 3 and 7, transfection with WISP1-siRNA; no. 2; 4 and 8, transfection with WISP2-siRNA no. 2. Data are expressed as mean ± SD of five experiments. (b) Expression level of WISP2 mRNA at 28 days after weekly transfection of WISP2-siRNA. (c) Percentages of albumin-positive cells. (d) Percentages of periodic acid–Schiff (PAS)-positive cells. (e) Urea production in the media.

was more densely stained in these cells. PAS staining showed that WISP2-siRNA combined with HGF/aFGF/bFGF/collagen coating induced much glycogen deposition in hepatocyte-like cells (Fig. 6e), whereas glycogen-stored cells were much fewer in the cells of 10% FBS/non-coated condition (Fig. 6f).

DISCUSSION

IN THE PRESENT study, we examined two steps to study the conditions to induce hepatic differentiation. First, the effect of combination of cytokines and 5-aza on hepatic differentiation was studied. 5-aza was used because cardiomyogenic differentiation of murine bone marrow stromal cells was approximately 30% by 5-aza.[14] Treatment with 5-aza and bFGF actually caused hepatic differentiation, judging from expression of albumin as well as other liver-specific genes. Hence, demethylation of genes may be important for differentiation of MSC. The cytokines whose receptors were expressed were used (data not shown). During embryonic development, the production of growth factors such as HGF and FGF has been associated with endoderm specification.[19,20] In addition, HGF may be an important regulator in the early stage of hepatogenesis, as HGF plays a role in regeneration of acute hepatitis.[21] Second, the combined effects of cytokines and type IV collagen coating were examined, because type IV collagen was the most potent inducer of colonization of hepatic progenitor cells.[10] The importance of the extracellular matrix in the liver developmental process has increasingly been recognized.[22] Undifferentiated mouse ES cells express integrins α6, β1, β4, β5, laminin receptor 1 and dytroglycan, and are thus poised to receive signals from the extracellular matrix.[23] Mouse hepatic progenitor cells in fetal liver express CD49f (α6 inetgrin) and CD29 (β1 integrin), and these cells respond well to type IV collagen.[10] E7T-13 cells were reported to express CD29 and CD49,[12] and these molecules may be important for hepatic differentiation.

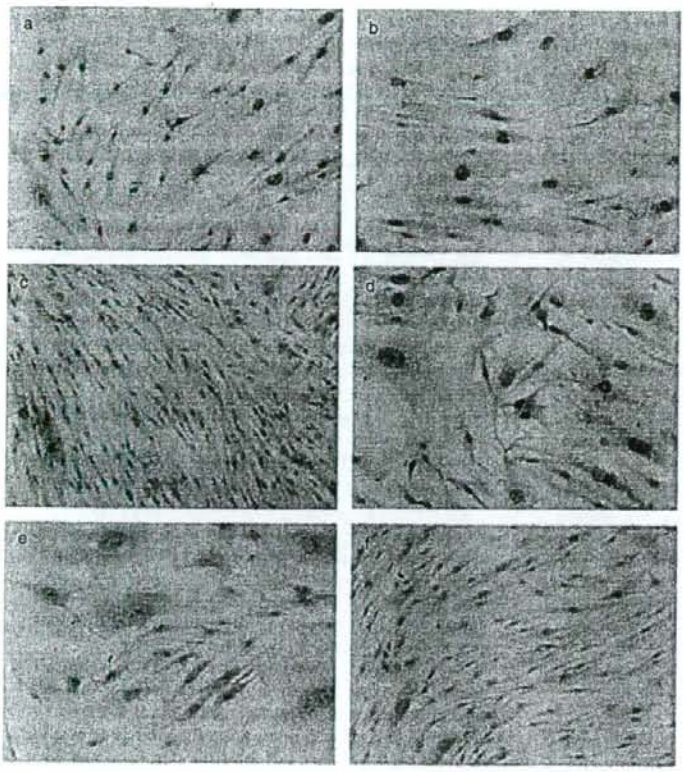

Figure 6 Cytochemical analysis of the cells. (a) UE7T-13 cells cultured in 10% fetal bovine serum (FBS)/non-coated condition with transfection of WISP1-siRNA (albumin staining, original magnification ×200). (b) UE7T-13 cells cultured in 10% FBS/non-coated condition with transfection of WISP2-siRNA (albumin staining, original magnification ×200). (c) UE7T-13 cells cultured in 10% FBS/non-coated condition with transfection of non-silencing control siRNA (albumin staining, original magnification ×200). (d) UE7T-13 cells cultured in HGF/aFGF/bFGF/collagen-coated condition with transfection of WISP1-siRNA (albumin staining, original magnification ×200). (e) UE7T-13 cells cultured in HGF/aFGF/bFGF/collagen-coated condition with transfection of WISP2-siRNA (periodic acid–Schiff [PAS] staining, original magnification ×200). (f) UE7T-13 cells cultured in 10% FBS/non-coated condition with transfection of non-silencing control siRNA (PAS staining, original magnification ×200).

In the present study, downregulation of *WISP1* and *WISP2* during hepatic differentiation was observed. Knockdown experiments of these genes confirmed the critical roles of these genes in hepatic differentiation of MSC. *WISP1* and *WISP2* belong to the CCN family, which are involved in the control of cell proliferation and differentiation by participating in internal and external cell signaling.[17] The CCN family include *CYR61* (*CCN1*), *CTGF* (*CCN2*), *NOV* (*CCN3*), and *ISP*-1 (*CCN4*), *WISP*-2 (*CCN5*) and *WISP*-3 (*CCN6*). *WISP1* and *WISP2* are downstream in the WNT1/β-catenin signaling pathway. *WISP2* was identified as a regulator of osteoblast function.[24] Interestingly, differential expression of CCN family genes in bone marrow-derived MSC during osteogenic, chondrogenic and adipogenic differentiation was observed.[25] *WISP2* expression declined during adipogenic differentiation, and *WISP3* expression was markedly reduced in chondrogenic differentiation. In addition, both WISP1 and CCN1 were reported to be an osteoblastic regulator of MSC during skeletal development and fracture repair.[16,18] These reports suggest that the CCN family proteins are important regulators of differentiation of MSC. MRP-1/CD9, which downregulates several *Wnt* family genes including *WISP1*, *WISP3* and *c-myc*, has been reported to suppress cell transformation including epithelial to mesenchymal transition through downregulation of Wnt.[26] In this context, one possible mechanism responsible for hepatic differentiation of MSC by WISP1 and WISP2 may be associated with mesenchymal epithelial transition.

Human bone marrow MSC are easy to isolate but difficult to study because of their limited life span. The advantages of using UE7T-13 cells in the repopulation study are as follows; the cells have the same expression pattern of surface markers with parental H4-1 cells,

UE7T-13 cells differentiate into cardiomyocytes and neuronal cells without affecting differentiation potential, UE7T-13 cells do not transform; they do not generate tumors in immunosuppressed mice, they do not form foci *in vitro*, and they stop dividing after confluence.[12,15] However, concerns regarding the use of the cells, to which *E7* and *hTERT* genes are introduced for human liver repopulation study, may be raised. In future studies, we will apply the technologies, which were obtained from the present study, to primary cultured human MSC, which are not genetically manipulated.

REFERENCES

1 Theise ND, Nimmmakakalu M, Gardner R *et al.* Liver from bone marrow in human. *Hepatology* 2000; **31**: 235–40.
2 Lagasse E, Conners H, Al-Dhalimy M *et al.* Purified hematopoietic stem cells can differentiate into hepatocytes in vivo. *Nat Med* 2000; 6: 1229–34.
3 Krause DS, Theise ND, Collector MI *et al.* Multi-organ, multi-lineage engraftment by a single bone marrow-derived stem cell. *Cell* 2001; **105**: 369–77.
4 Alison MR, Poulsom R, Jeffery R *et al.* Hepatocytes from non-hepatic adult stem cells. *Nature* 2000; **406**: 257.
5 Korbling M, Katz RL, Khanna A *et al.* Hepatocytes and epithelial cells of donor origin in recipients of peripheral-blood stem cells. *N Engl J Med* 2002; **346**: 738–46.
6 Jiang Y, Jahagirdar BN, Reinhardt RL *et al.* Pluripotency of mesenchymal stem cells derived from adult marrow. *Nature* 2002; **418**: 41–9.
7 Schwartz RE, Reyes M, Koodie L *et al.* Multipotent adult progenitor cells from bone marrow differentiate into functional hepatocyte-like cells. *J Clin Invest* 2000; **109**: 1291–302.
8 Lee K-D, Kuo TK, Wang-Peng J *et al.* In vitro hepatic differentation of human mesenchymal stem cells. *Hepatology* 2004; **40**: 1275–84.
9 Fausto N. Liver regeneration and repair: hepatocytes, prognostic cells, and stem cells. *Hepatology* 2004; **39**: 1477–87.
10 Suzuki A, Zheng Y-W, Kondo R *et al.* Flow-cytometric separation and enrichment of hepatic progenitor cells in the developing mouse liver. *Hepatology* 2000; **32**: 1230–9.
11 Reya T, Duncan AW, Domes J *et al.* A role for Wnt signalling in self-renewal of haematopoietic stem cells. *Nature* 2003; **423**: 409–14.
12 Takeda Y, Mori T, Imabayashi H *et al.* Can the life span of human marrow stromal cells be prolonged by bmi-1, E6, and E7 and/or telomerase without affecting cardiomyogenic differentiation? *J Gene Med* 2004; 6: 833–45.
13 Lee OK, Kuo TK, Chen W-M, Lee KD, Hsieh SL, Chen T. Isolation of multipotent mesenchymal stem cells from umbilical cord blood. *Blood* 2004; **103**: 1669–75.
14 Makino S, Fukuda K, Miyoshi S *et al.* Cardiomyocytes can be generated from marrow stromal cells in vitro. *J Clin Invest* 1999; **103**: 697–705.
15 Mori T, Kiyono T, Imabayashi HT *et al.* Combination of hTERT and bmi-1, E6, or E7 induces prolongation of the life span of bone marrow stromal cells from an elderly donor without affecting their neurogenic potential. *Mol Cell Biol* 2005; **25**: 5183–95.
16 Kang Q, Liu HH, Park JK *et al.* CCN1/Cyr61 is regulated by the canonical Wnt signal and plays an important role in Wnt3A-induced osteoblast differentiation of mesenchymal stem cells. *Mol Cell Biol* 2006; **26**: 2955–64.
17 Perbal B. CCN proteins: multifunctional signaling regulators. *Lancet* 2004; **363**: 62–4.
18 French DM, Kaul RJ, D'Souza AL *et al.* WISP-1 is an osteoblastic regulator expressed during skeletal development and fracture repair. *Am J Pathol* 2004; **165**: 855–67.
19 Schmidt C, Bladt F, Goedecke S *et al.* Scatter factor/hepatocyte growth factor is essential for liver development. *Nature* 1995; **373**: 699–702.
20 Jung J, Zheng M, Goldfarb M, Zaret K. Initiation of mammalian liver development from endoderm by fibroblast growth factors. *Science* 1999; **284**: 1998–2003.
21 Shiota G, Okano J, Kawasaki H, Kawamoto T, Nakamura T. Serum hepatocyte growth factor levels in liver diseases: clinical implications. *Hepatology* 1995; **21**: 106–12.
22 Shiojiri N, Sugiyama Y. Immunolocalization of extracellular matrix components and integrins during mouse liver development. *Hepatology* 2004; **40**: 346–55.
23 Ivanova N, Dimos J, Schaniel C, Hackney J, Moore K, Lemischka I. A stem cell molecular signature. *Science* 2002; **298**: 601–4.
24 Kumar S, Hand AT, Connor JR *et al.* Identification and cloning of a connective tissue growth factor-like cDNA from human osteoblasts encoding a novel regulator of osteoblast function. *J Biol Chem* 1999; **274**: 17123–31.
25 Schutze N, Noth U, Schneidreit J *et al.* Differential expression of CCN-family members in primary human bone marrow-derived mesenchymal stem cells during osteogenic, chondrogenic and adiopogenic differentaition. *Cell Commun Signal* 2005; **3**: 1–12.
26 Huang CL, Liu D, Masuya D *et al.* MRP-1/CD9 gene transduction downregulates Wnt signal pathways. *Oncogene* 2004; **23**: 7475–83.

EXPERIMENTAL CELL RESEARCH 313 (2007) 2550–2562

available at www.sciencedirect.com

ScienceDirect

www.elsevier.com/locate/yexcr

Research Article

'Working' cardiomyocytes exhibiting plateau action potentials from human placenta-derived extraembryonic mesodermal cells

Kazuma Okamoto[a,b], *Shunichiro Miyoshi*[c,d], *Masashi Toyoda*[a], *Naoko Hida*[a,c], *Yukinori Ikegami*[c], *Hatsune Makino*[a], *Nobuhiro Nishiyama*[c], *Hiroko Tsuji*[a,f], *Chang-Hao Cui*[a], *Kaoru Segawa*[e], *Taro Uyama*[a], *Daisuke Kami*[a], *Kenji Miyado*[a], *Hironori Asada*[f], *Kenji Matsumoto*[g], *Hirohisa Saito*[g], *Yasunori Yoshimura*[f], *Satoshi Ogawa*[c], *Ryo Aeba*[b], *Ryohei Yozu*[b], *Akihiro Umezawa*[a,*]

[a]*Department of Reproductive Biology and Pathology, National Research Institute for Child Health and Development, Tokyo, Japan*
[b]*Department of Surgery, Keio University School of Medicine, Tokyo, Japan*
[c]*Cardio-pulmonary Division of Keio University School of Medicine, Tokyo, Japan*
[d]*Institute for Advanced Cardiac Therapeutics, Keio University School of Medicine, Tokyo, Japan*
[e]*Department of Microbiology and Immunology, Keio University School of Medicine, Tokyo, Japan*
[f]*Department of Obstetrics and Gynecology, Keio University School of Medicine, Tokyo, Japan*
[g]*Department of Allergy and Immunology, National Research Institute for Child Health and Development, Tokyo, Japan*

ARTICLE INFORMATION

Article Chronology:
Received 24 August 2006
Revised version received
19 April 2007
Accepted 24 April 2007
Available online 5 May 2007

Keywords:
Placenta
Co-culture
Cardiac differentiation

ABSTRACT

The clinical application of cell transplantation for severe heart failure is a promising strategy to improve impaired cardiac function. Recently, an array of cell types, including bone marrow cells, endothelial progenitors, mesenchymal stem cells, resident cardiac stem cells, and embryonic stem cells, have become important candidates for cell sources for cardiac repair. In the present study, we focused on the placenta as a cell source. Cells from the chorionic plate in the fetal portion of the human placenta were obtained after delivery by the primary culture method, and the cells generated in this study had the Y sex chromosome, indicating that the cells were derived from the fetus. The cells potentially expressed 'working' cardiomyocyte-specific genes such as cardiac myosin heavy chain 7β, atrial myosin light chain, cardiac α-actin by gene chip analysis, and Csx/Nkx2.5, GATA4 by RT-PCR, cardiac troponin-I and connexin 43 by immunohistochemistry. These cells were able to differentiate into cardiomyocytes. Cardiac troponin-I and connexin 43 displayed a discontinuous pattern of localization at intercellular contact sites after cardiomyogenic differentiation, suggesting that the chorionic mesoderm contained a large number of cells with cardiomyogenic potential. The cells began spontaneously beating 3 days after co-cultivation with murine fetal cardiomyocytes and the frequency of beating cells reached a maximum on day 10. The contraction of the cardiomyocytes was rhythmical and synchronous, suggesting the presence of electrical communication between the cells. Placenta-derived human fetal cells may be useful for patients who cannot supply bone marrow cells but want to receive stem cell-based cardiac therapy.

* *Corresponding author.* Fax: +81 3 5494 7048.
E-mail address: umezawa@198S.jukuin.keio.ac.jp (A. Umezawa).

0014-4827/$ – see front matter © 2007 Elsevier Inc. All rights reserved.
doi:10.1016/j.yexcr.2007.04.028

Introduction

Major advances have been made in the prevention, diagnosis, and treatment of ischemic heart disease and cardiomyopathy, including the use of heart transplantation and artificial hearts. However, the number of patients suffering from heart disease is still increasing [1]. Morbidity and mortality from cardiovascular diseases continue to be an enormous burden experienced by many individuals, with substantial economic cost. Enthusiasm for cell therapy for the injured heart has already reached the clinical setting, with physicians in several countries involved in clinical trials using several types of cell populations [2,3]. Bone-marrow-derived mononuclear cells [4,5], unfractioned bone marrow cells [6], bone-marrow-derived CD133$^+$ cells [7], and myoblasts [8] have been injected into the ischemic heart clinically.

Mesenchymal stem cells (MSCs) are a potential cellular source for stem cell-based therapy, since they have the ability to proliferate and differentiate into mesodermal tissues, including the heart tissue, and entail no ethical problems [9]. Human MSCs have been used clinically to treat patients with graft versus host disease and osteogenesis imperfecta [10,11]. We previously showed that murine and human marrow-derived MSCs can differentiate into cardiomyocytes and start to beat synchronously in vitro [12,13]. In addition, we and other groups proposed that direct injection of murine MSCs into the heart is a feasible approach in murine models of ischemic heart disease and in the normal mouse heart [14,15]. Although MSC transplantation slightly improved impaired cardiac function, this effect was limited. One of the reasons for this may be due to an extremely low rate of cardiomyogenesis from marrow-derived MSCs in vitro [13] and in vivo [14–17]. In order to further improve cardiac function, we have been searching for another source of MSCs having highly cardiomyogenic potential.

The placenta is composed of the amniotic membrane, chorionic mesoderm, and decidua; the amniotic membrane and chorionic mesoderm are the fetal portion and the decidua is the maternal portion (Fig. 1A) [18]. Recently it was reported that the chorionic villi of the placenta differentiated into osteocytes, chondrocytes and adipocytes under specific culture conditions [19,20]. In this study, we generated cells with the mesenchymal phenotype from the chorionic mesoderm, and

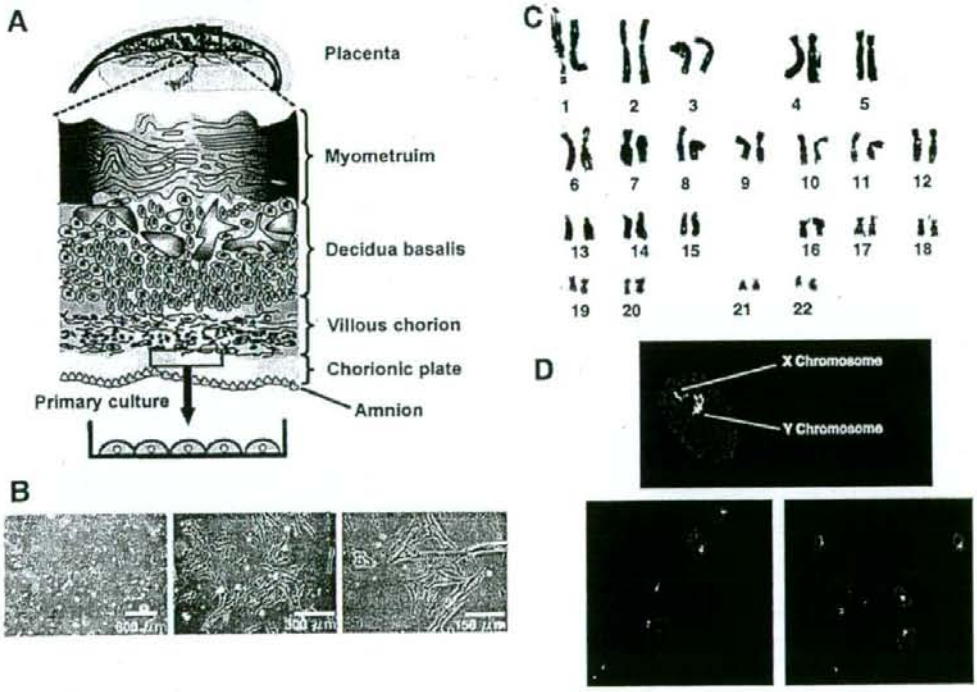

Fig. 1 – Establishment of chorionic plate cells. (A) Chorionic plate cells were established by primary culture of chorionic plate (red square in the chorionic mesoderm) in the human placenta. (B) Chorionic plate cells at PD 4 consisted of heterogeneous cell population. Three images show chorionic plate cells in the same culture dish. Their shape is different from that of fibroblasts. (C) Karyotyping by G-banding stain of chorionic plate cells. No chromosomal aberration was detected. (D) Chorionic plate cells have one X chromosome (red) and one Y chromosome (light blue). Nuclei were stained with DAPI (blue). (E) Flowcytometric analysis of chorionic plate cells using antibodies for CD14, CD29, CD31, CD34, CD44, CD45, CD59, CD73, CD90, CD105 and CD166. Black lines and shaded areas indicate reactivity of antibodies for isotype controls and that of antibodies for cell surface markers, respectively.

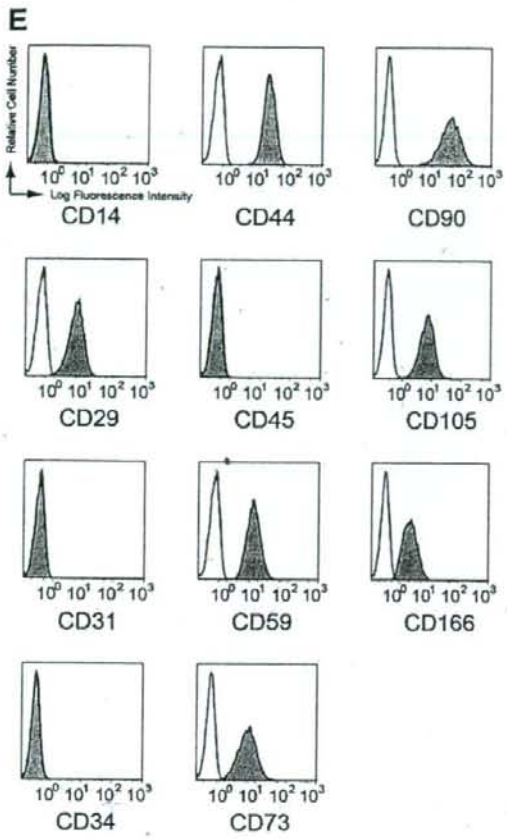

Fig. 1 (*continued*).

showed that: (a) physiologically functioning cardiomyocytes were transdifferentiated from human placenta-derived chorionic plate cells, but clear osteogenic and adipogenic phenotypes were not induced; (b) the cardiomyogenic induction rate obtained using our system was relatively high compared to that obtained using the previously described method [13]; (c) cocultivation with fetal murine cardiomyocytes alone without transdifferentiation factors such as 5-azaC or oxytocin is sufficient for cardiomyogenesis in our system; (d) chorionic plate cells have the electrophysiological properties of 'working' cardiomyocytes. The chorionic mesoderm contained a large number of cells with a cardiomyogenic potential.

Materials and methods

Chorionic plate cell culture

A human placenta was collected after delivery of a male neonate with informed consent. The study was approved by the ethics committee of Keio University, Tokyo, Japan (Number 17-44-1). To isolate chorionic plate cells, we used the explant culture method, in which the cells were outgrown from pieces of chorionic plate attached to dishes (Fig. 1A). Briefly, the decidua of the maternal part was separated and discarded. The chorionic plate from the fetal part were cut into pieces approximately 5 mm^3 in size. The pieces were washed in DMEM (high glucose; Kohjin Bio) supplemented with 100 U/ml penicillin–streptomycin (Gibco), 1 μg/ml Amphotericin B (Gibco) and 4 U/ml Novo-Heparin Injection 1000 (Mochidaseiyaku Co., Ltd.), until the supernatant was free of erythrocytes. Some pieces of chorionic plate were attached to the substratum in a 10-cm-diameter dish (Falcon, Becton, Dickinson and Company (BD), San Jose, CA, USA). Culture medium consisting of DMEM (high glucose; Kohjin Bio) supplemented with 10% FBS (CCT, Cansera, Canada) was added. The cells migrated out from the cut ends after approximately 20 days of incubation at 37 °C in 5% CO_2. The migrated cells were harvested with phosphate-buffered saline (PBS) with 0.1% trypsin and 0.25 mM EDTA (ethylenediamine-N,N,N',N'-tetraacetic acid) (Immuno-Biological Laboratories) for 5 min at 37 °C and counted. The harvested cells were re-seeded at a density of 3×10^5 cells in a 10-cm-diameter dish. Confluent monolayers of cells were subcultured at a 1:8 split ratio onto new 10-cm-diameter dishes and designated "chorionic plate cells". The culture medium was replaced with fresh culture medium every 3 or 4 days. The chorionic plate cells used in this study were within five to nine population doublings (approximately two to five passages).

Reverse transcriptase (RT)-PCR

Chorionic plate cells at PD 6 were dissociated with 0.1% trypsin and 0.25 mM EDTA for 5 min at 37 °C. Total RNA was extracted with RNeasy (Qiagen). Human cardiac RNA was purchased (Clontech). RNA for RT-PCR was converted to cDNA with Superscript (Invitrogen) according to the manufacturer's recommendations. RT-PCR was performed by using primers for the genes of cardiac transcription factors: Csx/Nkx-2.5, GATA4; a cardiac hormone: atrial natriuretic peptide (ANP), brain natriuretic peptide (BNP); cardiac structural proteins: cardiac troponin-I (cTnI), cardiac troponin T (cTnT), myosin light chain-2α (MLC-2α), cardiac actin; and 18s rRNA. 18s rRNA (18S) was used as an internal control. PCR was performed with recombinant Taq (Toyobo Co., Ltd.) or TaKaRa LA Taq with GC Buffer (Takara Shuzo Co., Ltd.) for 30 or 35 cycles, with each cycle consisting of 95 °C for 30 s, 55 °C, 61 °C or 65 °C for 45 s, and 2 °C for 45 s, with an additional 5-min incubation at 72 °C after completion of the final cycle. The PCR was performed in 50 μl of buffer (10 mmol/l Tris–HCl (pH 8.3), 2.5 mmol/l $MgCl_2$, and 50 mmol/l KCl) containing 1 mmol/l each of dATP, dCTP, dGTP, and dTTP, 2.5 U of Gene Taq (Nippon Gene), and 0.2 mol/l primers. The PCR products were size fractionated by 2% agarose gel electrophoresis.

Karyotyping of chorionic plate cells

Metaphase spreads were prepared from chorionic plate cells treated with 100 ng/ml colcemid (Karyo Max, Gibco Co. BRL) for 6 h. We performed karyotyping by G-banding stain on at least 30 metaphase spreads for each population. The CEP X/Y DNA Probe Kit (Vysis) was used to determine the proportion of XX and XY cells in accordance with the manufacturer's suggestions.

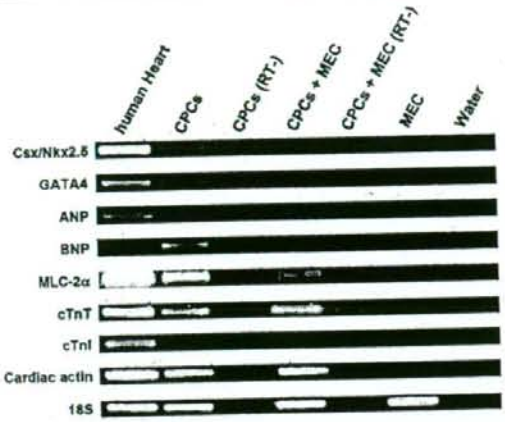

Fig. 2 – Gene expression of cardiomyocyte-specific/associated genes in chorionic plate cells. RT-PCR analysis revealed expression patterns of cardiomyocyte-specific or associated genes; *Csx/Nkx2.5, GATA4, ANP, BNP, cTnI, cTnT, cardiac actin* and *MLC-2α* (from left to right) in human heart, chorionic plate cells (CPCs), chorionic plate cells after co-culturing with murine embryonic cardiomyocytes (CPCs + MEC), murine embryonic cardiomyocytes (MEC) and water. "RT-" represented an omission of a reverse transcriptase treatment to RNA as negative control. Human heart RNA and water (without RNA) served as positive and negative control, respectively. 18s rRNA (18S) was amplified in parallel reactions as a housekeeping gene serving as an internal control.

Flow cytometric analysis

Chorionic plate cells were stained for 1 h at 4 °C with primary antibodies and immunofluorescent secondary antibodies. The cells were then analyzed on a Cytomics FC 500 (Beckman Coulter, Inc.) and the data were analyzed with the FlowJo Ver.7 (Tree Star, Inc.). Antibodies against human CD14 (6603511, Beckman Coulter), CD29 (Integrin-β1) (6604105, Beckman Coulter), CD31 (PECAM-1) (IM1431, Beckman Coulter), CD34 (IM1250, Beckman Coulter), CD44 (IM1219, Beckman Coulter, IM1219), CD45 (556828, Beckman Coulter), CD59 (IM3457, Beckman Coulter), CD73 (550257, BD Pharmingen), CD90 (Thy-1) (555596, BD Pharmingen), CD105 (Endoglin) (A07414, Beckman Coulter) and CD166 (ALCAM) (559263, BD Pharmingen) were adopted as primary antibodies.

Gene chip analysis

Human genomewide gene expression was examined with the Human Genome U133A Probe array (Affymetrix), which contains the oligonucleotide probe set for approximately 23,000 full-length genes and expressed sequence tags (ESTs). Total cellular RNA was immediately isolated with the RNeasy (Qiagen), according to the manufacture's instructions. Contaminating DNA was eliminated by DNase I (Takara Bio Inc.). The purity of RNA was assessed on the basis of the A260/A280 ratio, and the integrity of RNA was verified by agarose gel electrophoresis. Double-stranded cDNA was synthesized from DNase-treated total RNA, and the cDNA was subjected to in vitro transcription in the presence of biotinylated nucleoside triphosphates, according to the manufacturer's protocol (One-Cycle Target Labeling and Control Reagent package [http://www.affymetrix.com/support/technical/manual/expression_manual.affx]). The biotinylated cRNA was hybridized with a probe array for 16 h at 45 °C, and the hybridized biotinylated cRNA was stained with streptavidin-PE and scanned with a Hewlett-Packard Gene Array Scanner (Palo Alto). The fluorescence intensity of each probe was quantified by using the GeneChip Analysis Suite 5.0 computer program (Affymetrix). The expression level of a single mRNA was determined as the average fluorescence intensity among the intensities obtained with 11 paired (perfectly matched and single-nucleotide-mismatched) probes consisting of 25-mer oligonucleotides. If the intensities of mismatched probes were very high, gene expression was judged to be absent, even if high average fluorescence was obtained with the GeneChip Analysis Suite 5.0 program. The level of gene expression was determined with the GeneChip software as the average difference (AD). Specific AD levels were then calculated as the percentage of the mean AD level of six probe sets for housekeeping genes (actin and GAPDH [glyceraldehyde-3-phosphate dehydrogenase] genes). Further data analysis was performed with Genespring software version 5 (Silicon Genetics). To normalize the staining intensity variations among chips, the AD values for all genes on a given chip were divided by the median of all measurements on that chip. To eliminate changes within the range of background noise and to select the most differentially expressed genes, data were used only if the raw data values were less than 100 AD and gene expression was judged to be present by the Affymetrix data analysis.

Table 1 – RT-PCR primers used in this study

	Primer (sense)	Primer (anti-sense)	Annealing temperature (°C)	Product size (bp)
Csx/Nkx-2.5	CTTCAAGCCAGAGGCCTACG	CCGCCTCTGTCTTCTCCAGC	61	233
GATA4	GACGGGTCACTATCTGTGCAAC	AGACATCGCACTGACTGAGAAC	61	475
ANP	GAACCAGAGGGGAGAGACAGAG	CCCTCAGCTTGCTTTTTAGGAG	55	406
BNP	CATTTGCAGGGCAAACTGTC	CATCTTCCTCCCAAAGCAGC	55	206
MLC-2α	GAAGGTGAGTGTCCCAGAGG	ACAGAGTTTATTGAGGTGCCCC	65	376
cTnT	GGCAGCGGAAGAGGATGCTGAA	GAGGCACCAAGTTGGGCATGAACGA	65	152
cTnI	CCCTGCACCAGCCCCAATCAGA	CGAAGCCCAGCCCGGTCAACT	65	233
Cardiac actin	CTTCCGCTGTCCTGAGACAC	CCTGACTGGAAGGTAGATGG	61	400
18S	GTGGAGCGATTTGTCTGGTT	CGCTGAGCCAGTCAGTGTAG	55	200

Table 2 – Human cardiomyocyte-specific or -associated gene expression profiling of undifferentiated and differentiated chorionic plate cells (CPCs)

Systematic	Common	Undifferentiated CPCs		Differentiated CPCs		Human heart	Description
207317_s_at	CASQ2	34	A	12	A	P	Calsequestrin 2 (cardiac muscle)
205553_s_at	CSRP3	8	A	5	A	P	Cysteine and glycine-rich protein 3 (cardiac LIM protein)
208040_s_at	MYBPC3	56	A	117	A	P	Myosin binding protein C, cardiac
214468_at	MYH6	11	A	50	A	P	Myosin, heavy polypeptide 6, cardiac muscle, alpha (cardiomyopathy, hypertrophic 1)
204737_s_at	MYH7	5	A	161	P	P	Myosin, heavy polypeptide 7, cardiac muscle, beta
216265_x_at	MYH7	36	A	232	A	P	Myosin, heavy polypeptide 7, cardiac muscle, beta
215795_at	MYH7B	89	A	11	A	P	Myosin, heavy polypeptide 7B, cardiac muscle, beta
209742_s_at	MYL2	267	A	153	A	P	Myosin, light polypeptide 2, regulatory, cardiac, slow
210088_x_at	MYL4	338	P	404	A	P	Myosin, light polypeptide 4, alkali; atrial, embryonic
210395_x_at	MYL4	220	P	412	P	P	Myosin, light polypeptide 4, alkali; atrial, embryonic
219942_at	MYL7	9	A	16	A	P	Myosin, light polypeptide 7, regulatory
207557_s_at	RYR2	11	A	13	A	P	Ryanodine receptor 2 (cardiac)
214044_at	RYR2	17	A	23	A	P	Ryanodine receptor 2 (cardiac)
205742_at	TNNI3	96	A	195	A	P	Troponin I, cardiac
215389_s_at	TNNT2	83	A	165	A	P	Troponin T2, cardiac
205132_at	ACTC	289	P	671	P	P	Actin, alpha, cardiac muscle
206029_at	ANKRD1	214	P	13	A	P	Ankyrin repeat domain 1 (cardiac muscle)
213738_s_at	ATP5A1	5905	P	2657	P	P	ATP synthase, H^+ transporting, mitochondrial F1 complex, alpha subunit, isoform 1, cardiac muscle
205444_at	ATP2A1	107	A	53	A	A	ATPase, Ca^{++} transporting, cardiac muscle, fast twitch 1
209186_at	ATP2A2(SERCA2A)	4465	P	2577	P	P	ATPase, Ca^{++} transporting, cardiac muscle, slow twitch 2
212361_s_at	ATP2A2(SERCA2A)	814	P	338	A	P	ATPase, Ca^{++} transporting, cardiac muscle, slow twitch 2
212362_at	ATP2A2(SERCA2A)	178	P	60	A	A	ATPase, Ca^{++} transporting, cardiac muscle, slow twitch 2
207317_s_at	CASQ2	34	A	12	A	P	Calsequestrin 2 (cardiac muscle)
65472_at		6	A	17	A	A	qb80a04.x1 Soares_fetal_heart_NbHH19W *Homo Sapiens* cDNA clone IMAGE:1706382 3′ similar to TR:O21123 O21123 CYTOCHROME OXIDASE I; mRNA sequence
205298_s_at	BTN2A2	482	P	183	A	A	zd240d07.s1 Soares_fetal_heart_NbHH19W *Homo sapiens* cDNA clone IMAGE:341581 3′, mRNA sequence
213121_at	SNRP70	66	A	6	A	A	zd39c08.s1 Soares_fetal_heart_NbHH19W *Homo sapiens* cDNA clone IMAGE:343022 3′, mRNA sequence
65521_at	LOC51619	658	A	266	A	P	zd56g04.r1 Soares_fetal_heart_NbHH19W *Homo sapiens* cDNA clone IMAGE:344694 5′, mRNA sequence

214014_at	CDC42EP2	38	A	14	A	A	zd85d03.s1 Soares_fetal_heart_NbHH19W *Homo sapiens* cDNA clone IMAGE:347429 3', mRNA sequence
201204_s_at	RRBP1	2174	P	1257	P	P	zf44f12.s1 Soares_fetal_heart_NbHH19W *Homo sapiens* cDNA clone IMAGE:379823 3', mRNA sequence
209331_s_at	MAX	561	P	294	P	P	zg72g05.s1 Soares_fetal_heart_NbHH19W *Homo sapiens* cDNA clone IMAGE:398936 3', mRNA sequence
214776_x_at	XYLB	24	A	13	A	A	zi99g02.s1 Soares_fetal_liver_spleen_1NFLS_S1 *Homo sapiens* cDNA clone IMAGE:448946 3', mRNA sequence
211715_s_at	BDH	59	A	8	A	P	3-hydroxybutyrate dehydrogenase (heart, mitochondrial)
205534_at	PCDH7	8	A	205	P	A	BH-protocadherin (brain–heart)
205535_s_at	PCDH7	7	A	75	P	P	BH-protocadherin (brain–heart)
210273_at	PCDH7	157	A	168	A	P	BH-protocadherin (brain–heart)
210941_at	PCDH7	14	A	3	A	A	BH-protocadherin (brain–heart)
204726_at	CDH13	172	P	195	P	P	Cadherin 13, H-cadherin (heart)
203020_at	HHL	210	P	117	P	P	Expressed in hematopoietic cells, heart, liver
213982_s_at	HHL	335	P	74	P	P	Expressed in hematopoietic cells, heart, liver
205738_s_at	FABP3	79	A	92	P	P	Fatty acid binding protein 3, muscle and heart (mammary-derived growth inhibitor)
214285_at	FABP3	22	A	49	A	P	Fatty acid binding protein 3, muscle and heart (mammary-derived growth inhibitor)
220138_at	HAND1	246	A	117	A	P	Heart and neural crest derivatives expressed 1
220480_at	HAND2	19	A	29	A	A	Heart and neural crest derivatives expressed 2
213036_x_at	ATP2A3	23	A	25	A	A	*Homo sapiens* SERCA3 gene, exons 1–7 (and joined CDS)
204938_s_at	PLN	22	A	60	A	P	Phospholamban
204939_s_at	PLN	71	A	99	A	P	Phospholamban
204940_at	PLN	46	A	28	A	P	Phospholamban
206578_at	NKX2-5	40	A	14	A	P	NK2 transcription factor related, locus 5 (Drosophila)
205517_at	GATA4	16	A	46	A	P	GATA binding protein 4
201667_at	GJA1	4792	P	2016	P	P	Gap junction protein, alpha 1, 43 kDa (connexin 43)
208636_at	ACTN1	7896	P	3182	P	P	Actinin, alpha 1
208637_x_at	ACTN1	5400	P	2359	P	P	Actinin, alpha 1
211160_x_at	ACTN1	5727	P	1529	P	A	Actinin, alpha 1
203861_s_at	ACTN2	38	A	17	A	P	Actinin, alpha 2
203862_s_at	ACTN2	53	A	16	A	P	Actinin, alpha 2
203863_at	ACTN2	35	A	20	A	P	Actinin, alpha 2
203864_s_at	ACTN2	189	A	123	A	P	Actinin, alpha 2
206891_at	ACTN3	134	M	133	A	M	Actinin, alpha 3
200601_at	ACTN4	1134	P	282	P	P	Human non-muscle alpha-actinin mRNA, complete cds
211805_s_at	SLCBA1(NCX1)	53	A	228	A	P	Solute carrier family 8 (sodium/calcium exchanger), member 1
207413_s_at	SCN5A	32	A	61	A	P	Sodium channel, voltage-gated, type V, alpha (long QT syndrome 3)

Introduction of the EGFP gene

Recombinant adenovirus carrying the enhanced green fluorescent protein (EGFP) gene was prepared as described [13]. Chorionic plate cells were plated on dishes at $2\times10^5/cm^2$, and infected with EGFP-expressing adenovirus at 10 plaque-forming units/cell on the next day. Chorionic plate cells were examined in vitro by fluorescent confocal microscopy for expression of the EGFP gene. By 7 days post-infection, nearly all of the cells expressed EGFP. To eliminate the possibility of free adenovirus in the cell supernatant, we infected murine fetal cardiomyocytes with chorionic plate cell supernatants after infection. No murine fetal cardiomyocytes expressed EGFP, implying that the cells are not transfected with free adenovirus.

Preparation of murine fetal cardiomyocytes

Fetal cardiomyocytes were obtained from the hearts of day 17 mouse fetuses. The hearts were minced with scissors and washed with PBS, and then incubated in PBS with 0.1% trypsin and 0.25 mM EDTA for 10 min at 37 °C. After DMEM supplemented with 10% FBS was added, the cardiomyocytes were centrifuged at 1000 rpm for 5 min. The pellet was then re-suspended in 10 ml of DMEM with 10% FBS and incubated on glass dishes for 1 h to separate the cardiomyocytes from fibroblasts. The floating cardiomyocytes were collected and re-plated at $5\times10^4/cm^2$.

Co-culture system of chorionic plate cells and murine fetal cardiomyocytes

Neither 5-azaC [12] nor oxytocin [21] was used in this process as they are known to initiate cardiomyogenic differentiation. EGFP-labeled chorionic plate cells were harvested with 0.25% trypsin and 1 mM EDTA and overlaid onto the cultured fetal cardiomyocytes at $7\times10^3/cm^2$. Every 2 days the culture medium was replaced with fresh culture medium that was supplemented with 10% FBS and 1 μg/ml Amphotericin B (Gibco). The morphology of the beating EGFP-labeled chorionic plate cells was evaluated under a fluorescent microscope. The image was monitored using a CCD camera and stored as digital video. The cell contraction was analyzed using an image-edge detection program made by Igor Pro 4 (Wavemetrics Inc., Lake Oswego, Oregon).

Electrophysiological analysis

On day 10 of co-cultivation, action potentials (APs) were recorded as described previously [12,13] from spontaneously beating EGFP-labeled cells. Spontaneously beating EGFP-positive chorionic plate cells were selected as targets. The APs of the targeted cells had been recorded and Alexa568 dye was injected by iontophoresis to confirm that the APs were generated by EGFP-positive chorionic plate cells. The extent of dye transfer was monitored under a fluorescence microscope, and digital images were recorded with a digital photo camera (D100; Nikon, Tokyo, Japan) mounted on a microscope with a fluorescence filter (UMWIG2; Olympus).

Immunocytochemistry

A laser confocal microscope (LSM510, Zeiss) was used for immunocytochemical analysis. The chorionic plate cells co-cultured with fetal cardiomyocytes in vitro were fixed with 2% paraformaldehyde (PFA) in PBS for 20 min at 4 °C and treated with 0.1% Triton-X PBS for 20 min at room temperature. These cells were then stained with mouse monoclonal anti-human cardiac troponin-I antibody (#4T21/19-C7 HyTest, Euro, Finland) diluted 1:300, monoclonal anti-α-actinin antibody (Sigma) diluted 1:300, and anti-connexin 43 antibody (Sigma) diluted 1:300. To prevent fading and to stain nuclei, a Slow Fade Light Antifade kit with 4′-6-diamidino-2-phenylindole (DAPI) (Molecular Probes) was used.

Results

Establishment of chorionic plate cells

Almost all human tissues or organs can be a source of MSCs, which have been extracted from fat, muscle, menstrual blood, endometrium, placenta, umbilical cord, cord blood, skin, and eye. In this study, we focused on cells derived from fetuses, since fetus-derived cells tend to both differentiate and proliferate better than adult cells [22]. In that sense, human placenta is a good source of fetus-derived MSCs. We cultivated chorionic plate cells that were obtained from the chorionic mesoderm of the placenta (Fig. 1A). The chorionic plate cells regarded as being Population Doubling (PD) 0 or Day 0 were fibroblast-like in morphology, indistinguishable in appearance from the marrow-derived MSCs, and relatively larger in size than rapidly self-renewing stem cells [23] (Fig. 1B). The cells from PD 9 to PD 18 rapidly proliferated in culture and were propagated continuously. Chorionic plate cells did not undergo malignant transformation. They stopped dividing after reaching confluence and they did not form any foci after reaching confluence in vitro.

To clarify the character of the established chorionic plate cells, we first performed karyotypic analysis of 30 cells at PD 3. All cells had normal chromosomes without any chromosomal aberration (Fig. 1C). The sex chromosomes were found to be XY, implying that all cells were of fetal origin. Genomic FISH analysis also revealed that all cells had XY chromosomes (Fig. 1D). We examined the cell surface marker of the placenta-derived cells (chorionic plate cells) by FACS analysis (Fig. 1E). The surface markers of chorionic plate cells are exactly the same as those of previously reported bone-marrow- and cord blood-derived mesodermal cells, i.e., positive for CD29, CD44,

Fig. 3 – Immunocytochemistry of chorionic plate cells for human cardiac troponin-I. (A–F) Immunocytochemistry of differentiated chorionic plate cells with anti-human cardiac troponin-I (cTnI) antibody. The EGFP-positive cells (B) were stained with anti-human cTnI antibody (A) and the merged image (DAPI, EGFP, cTnI) is shown in panels D and F. An enlarged image (red square in D) is shown in panel E. Clear striations were observed with red fluorescence of cTnI in the differentiated cells. (G–I) A merged image for EGFP and cTnI is shown in panel G. A longitudinal section at the green line in the merged image G is shown in panel H. An axial section at the red line in merged image G is shown in panel I.

CD59, CD73, CD 90, CD105 and CD166, and negative for CD14, CD31, CD34 and CD45.

Next we investigated whether chorionic plate cells have cardiomyogenic potential by human cardiomyocyte-specific gene expression using RT-PCR method (Fig. 2, Table 1) and gene chip analysis (Table 2; GEO accession number, GSE7021: GSM162104 and GSM162105). Chorionic plate cells expressed Csx/Nkx-2.5, GATA4, BNP, cardiac troponin T (cTnT), cardiac